Journal of Alloys and Compounds 666 (2016) 248–253

Contents lists available at ScienceDirect

Journal of Alloys and Compounds

journal homepage: http://www.elsevier.com/locate/jalcom

Transition and transport behavior in spinel oxide $MgTi_2O_4$ and its La-doped counterparts

Yuanyuan Zhu [a, b], Rongjuan Wang [b], Li Wang [b], Yong Liu [b, **], Rui Xiong [b, *], Jing Shi [b], Mingliang Tian [a]

[a] High Magnetic Field Laboratory, Chinese Academy of Science, Shushanhu Road 350, Hefei 230031, Anhui, China
[b] Key Laboratory of Artificial Micro- and Nano-structures of Ministry of Education, School of Physics and Technology, Wuhan University, Wuhan 430072, China

ARTICLE INFO

Article history:
Received 2 December 2015
Received in revised form
3 January 2016
Accepted 8 January 2016
Available online 11 January 2016

Keywords:
$MgTi_2O_4$
Electrical transport
Transition

ABSTRACT

Spinel oxides $Mg_{1-x}La_xTi_2O_4$ ($x = 0$, 0.005, 0.01, and 0.015) were synthesized by spark plasma sintering. The temperature dependences of resistances were measured and investigated in details. It shows that the transition of $MgTi_2O_4$ occurs at T_t ~258 K, while the transition is weakening, and the transition temperature T_t decreases with La^{3+} doping. The fit of resistances versus temperature curves demonstrate that Mg_{1-x} $La_xTi_2O_4$ displays metal behavior above T_t, while a dual conducting mechanism, the Mott-insulator like variable range hopping (VRH) and normal activated conduction, should be responsible for the transport behavior of Mg_{1-x} $La_xTi_2O_4$ below T_t.

1. Introduction

Spinel compounds AB_2X_4, with the structure of AX_4 tetrahedra and BX_6 octahedra, have been studied for many years due to their fascinating physical properties. For example, $LiTi_2O_4$ shows superconductivity at $T_c = 11$ K [1,2]; LiV_2O_4 exhibits heavy fermion behavior [3–5]; ZnV_2O_4 and $ZnCr_2O_4$ display unusual magnetic and electric properties [6–9]; $MgTi_2O_4$ and $CuIr_2S_4$ experience spin-Peierls-like transition [10–12].

$MgTi_2O_4$ is a geometrically frustrated magnetic spinel compound with orbital ordered [11–16]. It is a potential candidate for single-valence dimerization due to the $3d^1$ electronic configuration of the oxidation state Ti^{3+}. With the decrease of temperature, $MgTi_2O_4$ is subjected to a structure phase transition at T_t ~260 K from cubic to tetragonal [11]. After phase transition, the magnetic behavior drops abruptly from Pauli paramagnetism to antiferromagnetism due to the simultaneous spin-dimer [13], accompanied by abnormal changes in electrical resistivity, thermal power, and optical reflectance [12–14].

However, the mechanisms for some behaviors of spinel oxide $MgTi_2O_4$ are still in debate. For example, about the transition phase, some researchers suggest that it is a first-order transition, based on their neutron diffraction results [11]. However, others thought it is a second-order transition, from the temperature dependence of X-ray diffraction experiments [13]. Another question is that the transport behavior of $MgTi_2O_4$ is still puzzling. Above T_t, the electrical resistivity of $MgTi_2O_4$ shows a small increase with temperature decreasing. There are several different explanations on this transport behavior. Zhou et al. thought that $MgTi_2O_4$ is a semiconductor above T_t, and the transition is from semiconductor to semiconductor. The explanation by Zhou et al. [12] is inconsistent with the results of magnetic susceptibility, which indicated that $MgTi_2O_4$ is a Pauli paramagnetism metal. Isobe et al. [13] suggest that the transition is still from metal to insulator, and the slow increase of electrical resistivity with decrease of temperature results from the grain boundary resistance.

In order to understand the underlying physical picture of the transport behavior of $MgTi_2O_4$ more clearly, further works on the transport behavior of $MgTi_2O_4$ are very necessary. For $MgTi_2O_4$, to the best of our knowledge, the A-site non-equivalent doping can effectively change the transport behavior but keep the characteristic of structure and transition as much as possible. In this work, we studied the temperature dependence of the transport behaviors of polycrystalline Mg_{1-x} $La_xTi_2O_4$ spinels with $x = 0$, 0.005, 0.01, 0.015. It was found that, La-doping has significant effects on the transition and transport properties. To our interest, in temperature

* Corresponding authors.
** Corresponding authors.
E-mail addresses: yongliu@whu.edu.cn (Y. Liu), xiongrui@whu.edu.cn (R. Xiong).

http://dx.doi.org/10.1016/j.jallcom.2016.01.062
0925-8388/

above T_t, the transport properties of all the polycrystalline $Mg_{1-x}La_xTi_2O_4$ can be well fitted by the contributions of both the grain and grain boundary resistances. However, the transport properties below T_t can be well explained with a dual mechanism: the Mott-insulator like variable range hopping (VRH) and normal activated conduction. Our results indicated that the transport behaviors of $MgTi_2O_4$ may result from the combined effects of different conduct mechanisms.

2. Experiments

Polycrystalline $Mg_{1-x}La_xTi_2O_4$ ($x = 0$, 0.005, 0.01, 0.015, 0.02, 0.03 and 0.05) compounds were prepared by spark plasma sintering (SPS) method, as referred in the previous work of our team [17]. Titanium trioxide (Ti_2O_3, Alfa, 99.8% purity), magnesia (MgO, Alfa, 99.95% purity) and lanthanum oxide (La_2O_3, Alfa, 99.99% purity) were used as the raw materials in this experiment. The mixture of MgO, La_2O_3 and Ti_2O_3 powders was charged into SPS graphite die with the diameter of 15 mm and a pressure of 4 KN was applied along Z-axis. After evacuating the SPS chamber (~10 Pa), the temperature was raised to 1300 K at a rate of 100 °C/min and kept for 1 h. The voltage and current were set to 3 V and 700 A, respectively. After sintering, the power supply was switching off and the temperature was decrease to room temperature. A pellet of $Mg_{1-x}La_xTi_2O_4$ with 15 mm in diameter and 2 mm in thickness was thus successfully prepared. *X*-ray diffraction (XRD) analysis was carried out with a scanning rate 0.01 s^{-1} with Cu Ka radiation (D8 Advanced, Bruker AXS, Germany). Resistance measurements were carried out in physical property measurement system (PPMS 6000, Quantum Design, USA) with usual four probe method.

3. Results and discussion

Fig. 1 displays the typical XRD patterns of $Mg_{1-x}La_xTi_2O_4$ polycrystalline samples with nominal concentrations of La^{3+} ions ($0 \le x \le 0.05$). The prominent peaks presented in Fig. 1 have with very small width at half maximum (FWHM), indicating the formation of the crystalline phase. For samples with $x < 0.02$, all the observed peaks are corresponding to the cubic spinel structure in $Fd\bar{3}m$ space group. In samples with $x = 0.02$–0.05, impurity phase of $LaTiO_3$ can be clearly observed, as denoted by the black solid ellipse dots in Fig. 1. The results indicate that the maximal nominal doping concentration is less than 0.02. Therefore, in this work, only those with $x \le 0.015$ were investigated.

In samples with $x \le 0.015$, only peaks belonging to cubic spinel

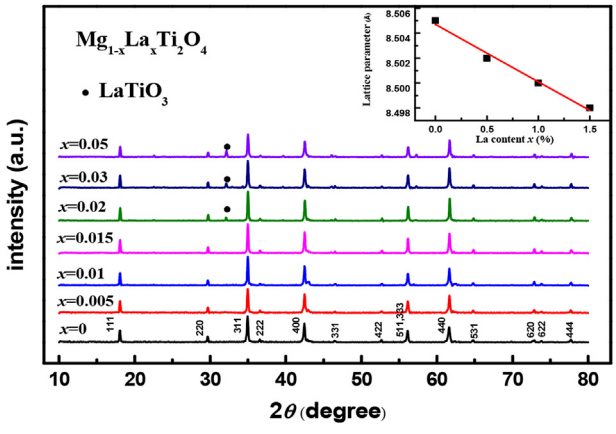

Fig. 1. XRD patterns for the series of $Mg_{1-x}La_xTi_2O_4$. The inset displays the dependence of the lattice constant on the La^{3+} ion concentration.

structure are observed, and with the increase of La^{3+} content ($0 \le x \le 0.015$), the positions of the peaks moves lightly toward to higher angles, which indicates that La^{3+} ions may be substituted for Mg^{2+} ions in the $MgTi_2O_4$ matrix. The lattice constant is calculated by a standard least-square fitting method from the XRD peaks and is shown in the inset of Fig. 1. It is found that the lattice constant decreases slightly with increasing La^{3+} ions content. The ionic radius of the La^{3+} and Mg^{2+} is 0.118 nm and 0.072 nm, respectively. According to the Vegard's law [18,19], the substituting La^{3+} for Mg^{2+} ions in the $MgTi_2O_4$ should expand the unit cell. However, in the spinel compounds $Mg_{1-x}La_xTi_2O_4$, three Mg^{2+} ions are replaced by two La^{3+} ions plus a vacancy based on the assumption that the Ti—O is not changed. This introduces a relatively large amount of structural vacancies, resulting in the lattice constant decreases with increasing La^{3+} ions content. As a result, Vegard's law is less important in such a situation. Besides that, the exchange between Mg-sites and Ti-sites also possibly plays a minor role for the observed phenomenon.

Fig. 2 shows the SEM images of the microstructure surface of $Mg_{1-x}La_xTi_2O_4$ prepared by SPS method. The crystal particles distribute compactly and the typical grain size is about 3 μm. It can be seen that the grain size is independent on La^{3+} content.

Fig. 3 shows the temperature dependence of electrical resistance (R) of $Mg_{1-x}La_xTi_2O_4$ with $x = 0$, 0.005, 0.01 and 0.015 in the temperature range from 5 to 300 K. For a more intuitive observation of the resistance change trend, the longitudinal axis in Fig. 3 is taken as the natural logarithm. It can be seen in Fig. 3, the electrical resistances of all the samples decrease with temperature increasing in the measured temperature range. For the pure $MgTi_2O_4$, a clear upward inflection near 258 K can be observed in the resistance versus temperature curve. In the temperature region above 258 K, the resistance is in an order of magnitude of ~10^{-1} Ω and increase slightly with temperature decreasing. As temperature goes below 258 K, the resistance increases sharply with the decrease of temperature and eventually reaches at a magnitude order of ~10^7 Ω. For the La^{3+} doped samples, the electrical resistance increases with the decrease of temperature in the whole temperature, just like that of pure $MgTi_2O_4$. It is observed that with the increase of La^{3+} doping content, the electrical resistances show slight increase as temperature is above 250 K, but decrease when temperature is below 250 K. The upward inflection apparently shown in R–T curve of pure $MgTi_2O_4$ is hard to distinguish in those of La-doped samples.

The upward inflection in the resistance versus temperature curve is observed near 258 K means that the transition of the pure $MgTi_2O_4$ occurs at 258 K. One question then issues: now that the upward inflection is hard to be observed in the La^{3+} doped samples, does the transition take place? To answer this question, the $d\ln(R/\Omega)/d(T/K)$ vs T curves in the vicinity of 258 K of all the samples were plotted in Fig. 4(a). It is found that all the three La^{3+}-doped samples show a peak in the $d\ln(R/\Omega)/d(T/K)$–T curves, just as that in the pure sample. It is noticed that the peak in the pure sample is sharp and steep, but the peaks for doped samples become much broader and lower. With the increase of the La^{3+} ion concentration, the peak position shift to lower temperature. The results indicate that the transition still takes place in La^{3+} doped samples, but the characteristic of the transition is weakening, and the transition temperature decreases with the increase of the La^{3+} ion concentration, as shown in Fig. 4(b). In $Mg_{1-x}La_xTi_2O_4$, Ti ions are expected to be in +3 valence state. When La enter the crystal as La^{3+} to replace Mg^{2+}, vacancies may be resulted due to requirement of the charge neutrality, and induce the distortion of the lattice. That may be also the origin of the decrease of lattice constant by La^{3+} ion doping. Thus, it is reasonable that the characteristic of the transition is weakening, and the temperature for the transition decreases with the increase of the La^{3+} ion concentration.

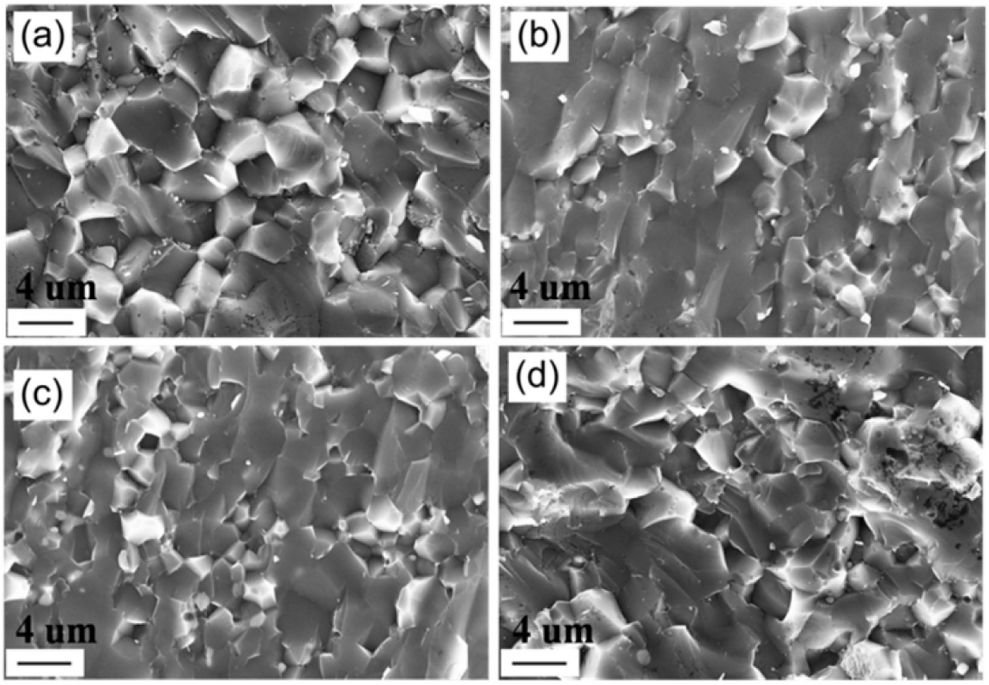

Fig. 2. The microstructure of the Mg_{1-x} $La_xTi_2O_4$ surface for a) $x = 0$, b) $x = 0.05$, c) $x = 0.01$, d) $x = 0.015$.

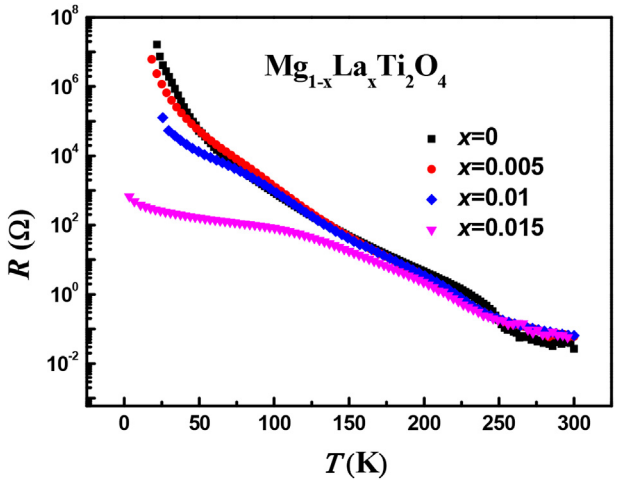

Fig. 3. Temperature dependence of resistances for the series of Mg_{1-x} $La_xTi_2O_4$.

The underlying mechanism for the transport behaviors of $MgTi_2O_4$ above the transition temperature is another interesting issue. The results show that the electrical resistivity of $MgTi_2O_4$ presents a small increase with temperature decreasing, indicating the semiconductor behavior. However, our attempts to fit the result using simple activated model fail. It implies that the transport behavior of $MgTi_2O_4$ above transition temperature has a complicated mechanism. Nevertheless, the previous work of Isobe et al. [13] presents that the conducting mechanism of $MgTi_2O_4$ above T_t is a metal. It is believed that the slow increase of electrical resistivity with decreasing temperature results from the grain boundary resistance. Besides that, a semi-conductive behavior and high resistivity have also been observed in a sintered sample of the typical metallic spinel oxide LiV_2O_4 [21]. As a result, we try to fit the temperature dependence of resistances above transition temperature of $MgTi_2O_4$ by considering two different contributions: one is from the contribution of the metal behavior; the other is from the contribution of the semi-conductor behavior, which is led by scattering of the grain boundaries.

Since the transition of doped and un-doped samples may begin around 270 K (see Fig. 4(a)), the fitting is chosen in a temperature range from 270 K to room temperature. In the fitting, the metallic resistances take the form of $R_1 = A + BT$, and the semi-conductor like resistance of the grain boundaries take the thermal excitation form of $R_2 = R_0\exp(\Delta E/k_BT)$, where k_B is the Boltzmann constant, and ΔE is the activation energy. Fig. 5(a–d) shows the fitting results for Mg_{1-x} $La_xTi_2O_4$ samples with $x = 0$, 0.005, 0.01 and 0.015, and the fitting parameters are shown in Table 1. It can be seen from Fig. 5 that the relationship between resistance and temperature above the transition temperature meets the formula of $R(T) = R_1 + R_2 = A + BT + R_0\exp(\Delta E/k_BT)$ very well. Our results strongly support the explanation of Isobe et al. [13] $MgTi_2O_4$ shows metal behavior above transition temperature. In Fig. 5, it is noticed that the $R–T$ curves for the semi-conductor behavior between the un-doped and La^{3+} doped samples show small difference: the activation energy for the four samples are all around 0.24 eV and the parameter R_0 have the same order of magnitudes; while big difference in metal-like resistance was observed between the un-doped and La^{3+} doped samples can be observed in that for the metal behavior: 1) The resistance of the un-doped $MgTi_2O_4$ at room temperature is lower than that of the doped sample. 2) Although both the undoped and doped samples show a cross temperature, at which the grains and the grain boundaries have equal resistance, the cross temperature decreases with the increase of doping content. 3) The fitted value B increases with the increase of doping content. In order to see the doping effect on the metal behavior more clear, we depict the curves of R_1/R_2 vs temperatures in Fig. 6. It is shown that the contribution of metal like resistance increase with the increase of doping concentration, indicating that the un-doped $MgTi_2O_4$ shows stronger metal behavior compare to the La^{3+} doped samples. These results can be understood in this way, as the doping concentration is very low, it can hardly influence the

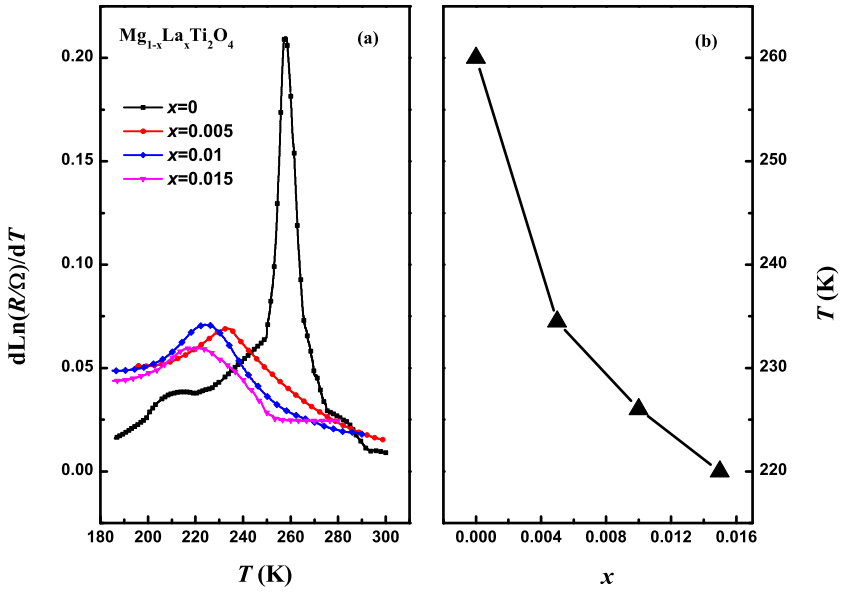

Fig. 4. (a) The dln(R/Ω)/d(T/K) curves as a function of temperature nearby T_t, (b) The T_t dependence of doping concentrations for Mg_{1-x} $La_xTi_2O_4$ system.

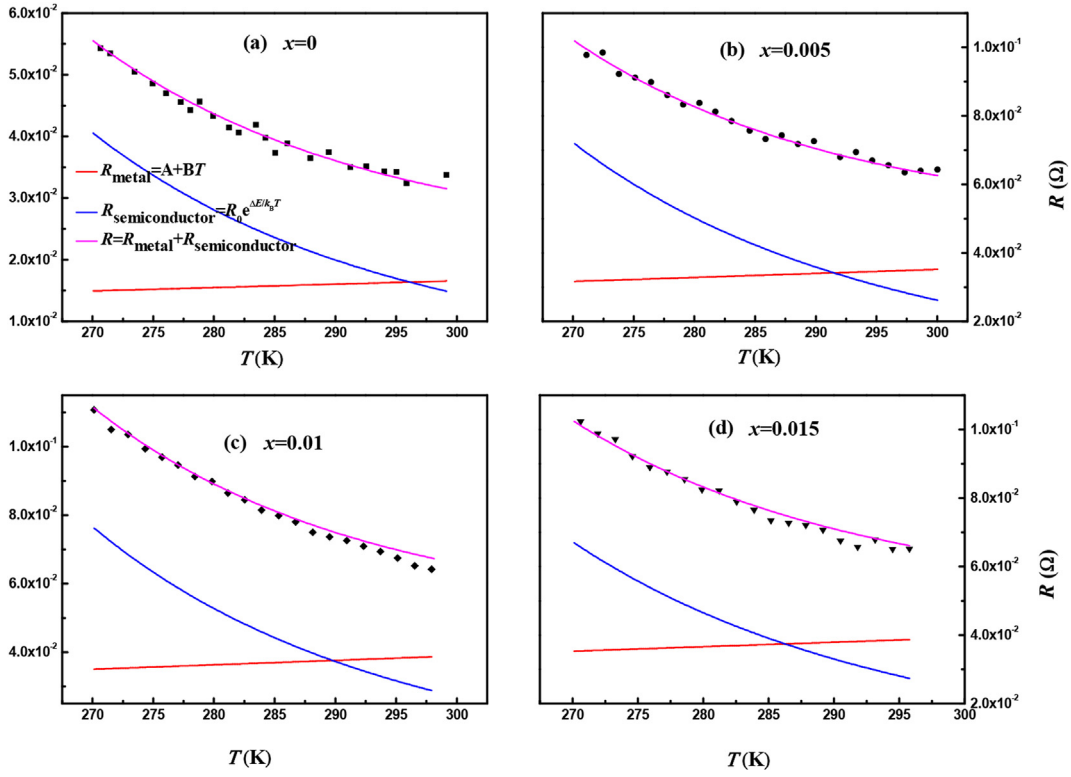

Fig. 5. Fitting results of the resistance versus temperature of Mg_{1-x} $La_xTi_2O_4$ above T_t, a) $x = 0$, b) $x = 0.05$, c) $x = 0.01$, d) $x = 0.015$. (The blue line and red line present the R semiconductor and R metal, respectively.). (For interpretation of the references to colour in this figure legend, the reader is referred to the web version of this article.)

Table 1
Parameters as calculated by the formula of $R = R_1+R_2 = A + BT + R_0e^{\Delta E/kBT}$.

Mg_{1-x} $La_xTi_2O_4$	A (Ω)	B (Ω/K)	ΔE (eV)	R_0 (Ω)
$X = 0$	7.54×10^{-18}	5.53×10^{-5}	0.239	1.37×10^{-6}
$x = 0.005$	1.49×10^{-17}	1.17×10^{-4}	0.236	3.05×10^{-6}
$x = 0.01$	5.84×10^{-18}	1.30×10^{-4}	0.242	2.26×10^{-6}
$x = 0.015$	9.41×10^{-18}	1.31×10^{-4}	0.240	2.24×10^{-6}

grain boundary, which means that the contribution of the scattering of the grain boundaries to the resistance in these un-doped and La-doped samples will be similar; the increase of vacancies leading by doping will change both the carrier concentration and the channel of carrier transport, so that significantly affect the conducting properties of the grain, resulting in a bad metal behavior for the La-doped samples: the fitted metal resistance is even larger than that of semi-conductor. The bad metal behavior in

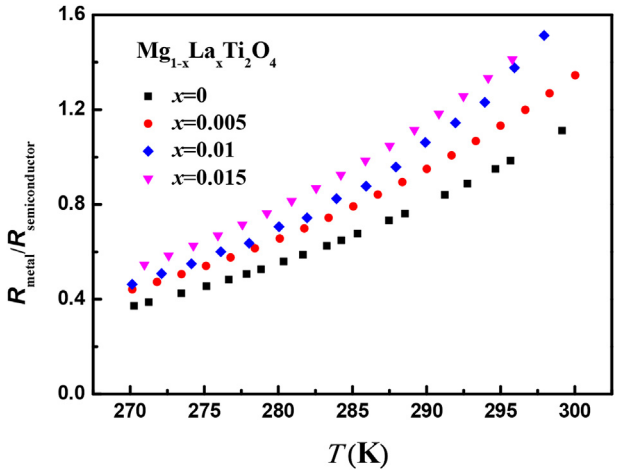

Fig. 6. The ratio of the R_1/R_2 ($R_1 = A + BT$, $R_2 = R_0 e^{\Delta E/kBT}$) for Mg_{1-x} $La_xTi_2O_4$ system (x = 0, 0.005, 0.01, 0.015).

La-doped samples offers further evidence of the metal behavior of $MgTi_2O_4$ in the temperature above transition. However, the grain–grain boundary model for high temperature region is just a presumption and further investigations should be taken to explain the transport phenomena of $MgTi_2O_4$ above T_t.

The rapid increasing resistance with decreasing temperature demonstrates the semiconducting state of $MgTi_2O_4$ below transition temperature without controversy. However, our attempts to fit the semiconducting state using simple activated model failed, implying that the semiconducting behavior of $MgTi_2O_4$ below transition temperature may also has a complicated mechanism. After careful analysis, we found that the resistance at low temperature show a change curvature in the Arrhenius plot ($\ln \sigma - 1/T$), which indicates a new conduction mechanism may account for it. We then tried to fit it with the Mott's variable range hopping (VRH) law $\sigma_{VRH} = Be^{-(T_0/T)^{1/4}}$, and found that VRH can fits the experimental data at low temperature. It seems that no single conduction model could accurately describe the semiconduct transport behavior of the sample over the entire temperature range below transition temperature. In order to explain the semiconducting behavior of $NdNiO_3$, a material undergoing a metal-insulator transition with temperature decreasing, G. Catalan et al. [20] have proposed a model by assuming that more than one transport mechanisms play roles simultaneously throughout the entire temperature range. Thus, instead, the transport behavior was fitted with a dual mechanism model in which the conductivity of the Mg_{1-x} $La_xTi_2O_4$ is considered to come from the contributions of both VRH and normal activated conduction:

$$\sigma = \sigma_A + \sigma_{VRH} = Ae^{-E_A/k_BT} + Be^{-(T_0/T)^{1/4}}$$

where E_A is thermal activated energy, k_B is Boltzman constant, T_0 is the hopping energy of three-dimensional variable range hopping (3D VRH). Considering that the thickness of the grain boundaries is much thinner than the size of grains, the contribution from the grain boundaries may play a minor role in low temperature region. Therefore, in the fitting, the effect of grain boundaries is ignored. Fig. 7 shows the fitting results (in the fitting, 180 K is chosen as the upper limit of temperature because the transition was found to end

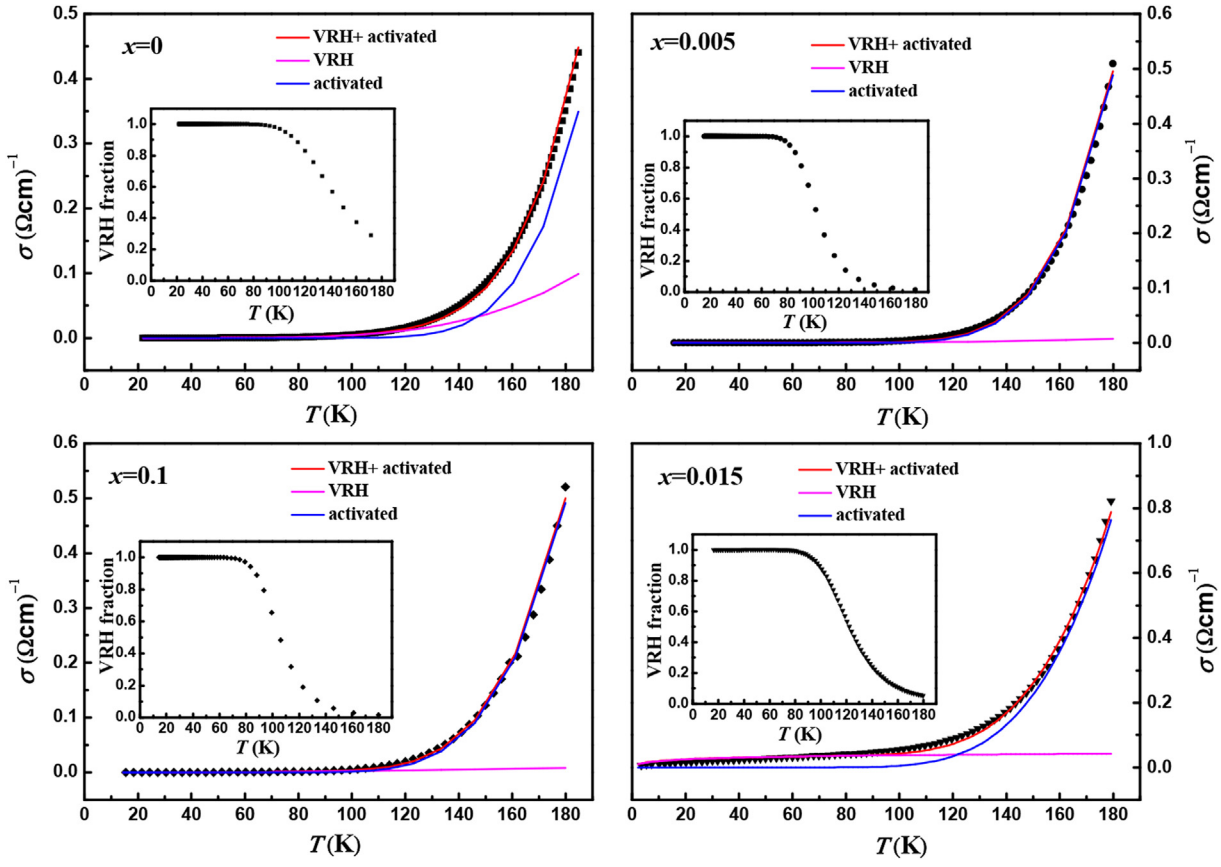

Fig. 7. Fitting results of conductivity versus temperature for Mg_{1-x} $La_xTi_2O_4$ (x = 0, 0.005, 0.01, 0.015) samples below T_t by two-mechanism model.

Table 2
Parameters as calculated by the two-mechanism model.

Mg_{1-x} $La_xTi_2O_4$	A (Scm^{-1})	E_A(eV)	B (Scm^{-1})	T_0(K)
$X = 0$	3758.58	0.148	1.36×10^7	2.28×10^7
$x = 0.005$	1644.42	0.126	1506.65	4.06×10^6
$x = 0.01$	761.25	0.114	15.45	5.83×10^5
$x = 0.015$	371.25	0.096	0.155	6.08×10^2

around this temperature, as shown in Fig. 4), and the fitting parameters are shown in Table 2. It was found the two-mechanism model describes the transport behavior of the Mg_{1-x} $La_xTi_2O_4$ very well in the temperature range. For un-doped $MgTi_2O_4$, the contribution from normal activated conduction is larger than that from VRH when temperature is above 150 K. As temperature decrease, the contribution from VRH becomes more and more important. Below 100 K, the conductivity almost all comes from the contribution of VRH. For the La^{3+} doped samples, similar conducting behaviors have been observed, except that the contribution of VRH plays an overwhelming role at lower temperature (about 80 K) and the fitting parameter T_0 reduces an order of magnitude with the increase of the La-doped content. To our notice, the fitting results for the doped sample with $x = 0.015$ have some different with that for $x = 0.005$ and 0.01, which might be come from the influence of $LaTiO_3$ impurity phase, tiny amount of $LaTiO_3$ may exist in the sample although it is not observed due to the resolution limit of XRD equipment.

In $MgTi_2O_4$, the dimer transition occurs simultaneously with the Peierls-like phase transition, due to the $3d^1$ electronic configuration of the oxidation state Ti^{3+}, and results in localization of free electron. The dimer transition is expected to play an important role in the transport properties. As a result, the localized electrons in Ti^{3+}–Ti^{3+} dimers participate in conducting following the law of Mott's variable range hopping. However, the dimerization extent of Ti^{3+} is strongly dependent on the temperature. Near the transition temperature, the extent of dimerization is weak, and the un-dimerized Ti^{3+} ions may participate in conducting following the law of thermal activated conduction.

In order to illustrate what extent VRH participates in the total conduction, we have plotted (inset in Fig. 7) the ratio between the VRH contribution and the total conduction. The results show that, for the pure $MgTi_2O_4$, the contribution of the VRH to the conducting increase from about 30% to 100% with temperature decrease from 170 K to 100 K. While for the La-doped samples ($x = 0.005$ and 0.01), the contribution of the VRH is about 30% at 130 K, and 100% as temperature goes below 80 K. These results strongly suggest that the A-side doping will result in the lowering of the dimerization extent of Ti^{3+}.

Based on the fitting results, we suggest that both the thermal activation conduction and three-dimensional variable range hopping conduction, which originates from the un-dimerization of Ti^{3+} ions and Ti^{3+}-Ti^{3+} dimers respectively, are accounting for the semiconducting behavior when temperature is below the transition temperature.

4. Conclusion

In summary, the transition and transport properties in $MgTi_2O_4$ and its La-doped counterparts were studied. While the transition in $MgTi_2O_4$ takes place at ~258 K, the transition is found to be suppressed somehow in the La-doped samples: the phase transition characteristic is weakening, and the transition temperature T_t decreases with the increase of La^{3+} doping content. In order to give a more general insight into the transport properties, the temperature dependences of resistance above and below T_t were fitted using different conducting mechanisms. The transport behaviors of Mg_{1-x} $La_xTi_2O_4$ system above T_t were well fitted by the contributions of both the metal-like grains and semiconduct-like grain boundaries. The transport behaviors of Mg_{1-x} $La_xTi_2O_4$ system below T_t result from the combined effects of the VRH and normal activated conduction, and the La^{3+} doping results in a decrease of the temperature at which VRH play a dominant role.

Acknowledgments

The authors would like to acknowledge the financial support from 973 Program (No. 2012CB821404), Chinese National Foundation of Natural Science (No. 11474224 and 11474225), National Science Fund for Talent Training in Basic Science (No. J1210061).

References

[1] D.C. Johnston, H. Prakash, W.H. Zachariasen, R. Viswanathan, Mater. Res. Bull. 8 (1973) 777.
[2] H.X. Geng, A.F. Dong, G.C. Che, Phys. C 432 (2005) 53.
[3] S. Kondo, D.C. Johnston, C.A. Swenson, F. Borsa, A.V. Mahajan, L.L. Miller, T. Gu, A.I. Goldman, M.B. Maple, D.A. Gajewski, E.J. Freeman, N.R. Dilley, R.P. Dickey, J. Merrin, K. Kojima, G.M. Luke, Y.J. Uemura, O. Chmaissem, J.D. Jorgensen, Phys. Rev. Lett. 78 (1997) 3729.
[4] N. Fujiwara, H. Yasuoka, Y. Ueda, Phys. Rev. B 57 (1998) 3539.
[5] C. Urano, M. Nohara, S. Kondo, F. Sakai, H. Takagi, T. Shiraki, T. Okubo, Phys. Rev. Lett. 85 (2000) 1052.
[6] Y. Ueda, N. Fujiwara, H. Yasuoka, J. Phys. Soc. Jpn. 66 (1997) 778.
[7] M. Reehuis, A. Krimmel, N. Büttgen, A. Loidl, A. Prokofiev, Eur. Phys. J. B 35 (2003) 311.
[8] S.H. Lee, D. Louca, H. Ueda, S. Park, T.J. Sato, M. Isobe, Y. Ueda, S. Rosenkranz, P. Zschack, J. Íñiguez, Y. Qiu, R. Osborn, Phys. Rev. Lett. 93 (2004) 156407.
[9] S.H. Lee, C. Broholm, T.H. Kim, W. Ratcliff, S.W. Cheong, Phys. Rev. Lett. 84 (2000) 3718.
[10] P.G. Radaelli, Y. Horibe, M.J. Gutmann, H. Ishibashi, C.H. Chen, R.M. Ibberson, Y. Koyama, Y.S. Hor, V. Kiryukhin, S.W. Cheong, Nature 416 (2002) 155.
[11] M. Schmidt, W. Ratcliff, P.G. Radaelli, K. Refson, N.M. Harrison, S.W. Cheong, Phys. Rev. Lett. 92 (2004) 056402.
[12] H.D. Zhou, J.B. Goodenough, Phys. Rev. B 72 (2005) 045118.
[13] M. Isobe, Y. Ueda, J. Phys. Soc. Jpn. 71 (2002) 1848.
[14] J. Zhou, G. Li, J.L. Luo, Y.C. Ma, D. Wu, B.P. Zhu, Z. Tang, J. Shi, N.L. Wang, Phys. Rev. B 74 (2006) 245102.
[15] Z.V. Popovic, G.D. Marzi, M.J. Konstantinovic, A. Cantarero, Z.D. Mitrovic, M. Isobe, Y. Ueda, Phys. Rev. B 68 (2003) 224302.
[16] H. Hoh, C. Kloc, E. Bucher, J. Solid State Chem. 125 (1996) 216.
[17] B.P. Zhu, Z. Tang, L.H. Zhao, L.L. Wang, C.Z. Li, D. Yin, Z.X. Yu, W.F. Tang, R. Xiong, J. Shi, X.F. Ruan, Mater. Lett. 61 (2007) 578.
[18] L. Vegard, Z. Phys. 5 (1921) 17.
[19] R. VidyaSagar, S. Buddhudu, Phys. Lett. A 373 (2009) 3184.
[20] G. Catalan, R.M. Bowman, J.M. Gregg, Phys. Rev. B 62 (2000) 12.
[21] K. Kawakami, Y. Sakai, N. Tsuda, J. Phys. Soc. Jpn. 55 (1986) 3174.